Journal of Alloys and Compounds 930 (2023) 167336

Contents lists available at ScienceDirect

Journal of Alloys and Compounds

journal homepage: www.elsevier.com/locate/jalcom

Ultra-low hysteresis in giant magnetocaloric $Mn_{1-x}V_xFe_{0.95}(P,Si,B)$ compounds

Jiawei Lai [a,b], Xinmin You [b], Jiayan Law [c], Victorino Franco [c], Bowei Huang [a,b], Dimitrios Bessas [d], Michael Maschek [b], Dechang Zeng [a,*], Niels van Dijk [b], Ekkes Brück [b,*]

[a] School of Materials Science & Engineering, South China University of Technology, Guangzhou 510640, China
[b] Fundamental Aspects of Materials and Energy, Department of Radiation Science and Technology, TU Delft, Mekelweg 15, 2629JB Delft, the Netherlands
[c] Dpto. Física de la Materia Condensada ICMSE-CSIC, Universidad de Sevilla, Apdo1065, 41080 Sevilla, Spain
[d] European Synchrotron Radiation Facility, F-38043 Grenoble, France

ARTICLE INFO

Article history:
Received 24 January 2022
Received in revised form 21 September 2022
Accepted 22 September 2022
Available online 30 September 2022

Keywords:
(Mn, V, Fe)1.95(P, Si,B)
Giant magnetocaloric effect
Magnetic properties
Entropy
Low hysteresis

ABSTRACT

Large thermal hysteresis in the $(Mn,Fe)_2(P,Si)$ system hinders an efficient heat exchange and thus limits the magnetocaloric applications. Substitution of manganese by vanadium in the $Mn_{1-x1}V_{x1}Fe_{0.95}P_{0.593}Si_{0.33}B_{0.077}$ and $Mn_{1-x2}V_{x2}Fe_{0.95}P_{0.563}Si_{0.36}B_{0.077}$ compounds enable a significant reduction in the thermal hysteresis without losing the giant magnetocaloric effect. For the composition closest to the critical one, where first-order crossovers to second-order phase transition in the series of x_2 = 0.02, $Mn_{0.98}V_{0.02}Fe_{0.95}P_{0.563}Si_{0.36}B_{0.077}$ exhibits a thermal hysteresis that is reduced from 1.5 to 0.5 K by 67%, yielding an adiabatic temperature change of 2.3 K and magnetic entropy change of 5.6 J/kgK for an applied field of 1 T, which demonstrates its potential for highly efficient magnetic heat pumps utilizing low-cost permanent magnets.

1. Introduction

Room temperature magnetic heat pumps attract broad attention due to their advantages compared to the traditional heat pumps, such as a high efficiency and a low impact on the environment [1,2]. Materials with a giant magnetocaloric effect (GMCE), which are the working materials of this technique, will release heat when an external magnetic field is applied, while they absorb heat when the magnetic field is removed. The performance of GMCE materials mainly determines the working efficiency and the cooling power of this technology. The GMCE usually occurs in materials that show a first-order magnetic transition (FOMT), such as $Gd_5Ge_2Si_2$, [3] $LaFe_{13-x}Si_x$, [4–7] $MnFeP_{1-x}As_x$, [8] $MnFeP_{1-x-y}Si_xB_y$, [9–11] $MnCoGe(Cu, B)_x$ [12,13] and Heusler [14] compounds. Among them, the $MnFeP_{1-x-y}Si_xB_y$ compounds are regarded as one of the most promising materials that can be industrialized because of their cheap and non-toxic elements, high cooling capacity and tunable T_C near room temperature [9].

$MnFeP_{1-x}Si_x$ compounds with a strong FOMT show a significant change in lattice parameters across the magnetic phase transition while keeping its hexagonal structure, which is a magneto-elastic transition [15]. However, a strong FOMT is often accompanied by large hysteresis, including both magnetic field hysteresis and thermal hysteresis (ΔT_{hys}), which will reduce field-induced temperature change. Hysteresis limits the practical application of these materials since it will largely reduce the working efficiency [16]. For some first-order materials that undergo a first-order magneto-structural transition, for instance Heusler alloys, the thermal hysteresis and magnetic field hysteresis may show a very different behavior. The magneto-structural transition is suppressed in field and thus a low hysteresis at low applied field and a lager hysteresis at high applied field could occur [17]. However, the presently studied $(Mn,Fe)_2(P,Si)$ based alloys undergo a magneto-elastic transition without a structural transition. In magneto-elastic transitions the thermal hysteresis and the magnetic field hysteresis are generally closely coupled, as reported previously [18]. We therefore consider that the low thermal hysteresis ΔT_{hys} is representative for a low magnetic field hysteresis, and thereby provides important information for the thermodynamic properties for magnetic heat pumps and magnetic refrigerators.

Theoretically, for a thermal hysteresis ΔT_{hys} of 2 K, the efficiency can be 60% of the Carnot efficiency and it can reach 75% of the Carnot efficiency if a value of 0.5 K is achieved [16]. Therefore, in the premise of keeping the GMCE, the thermal hysteresis should be made as narrow as possible by tailoring the microstructure or by tuning the

* Corresponding authors.
E-mail addresses: medczeng@scut.edu.cn (D. Zeng), E.H.Bruck@tudelft.nl (E. Brück).

https://doi.org/10.1016/j.jallcom.2022.167336

chemical composition. Recently, through 0.075 at% of B substitution in the $MnFe_{0.95}P_{0.595}Si_{0.33}B_{0.075}$ compounds, ΔT_{hys} can be optimized to 1.6 K according to the temperature-dependent magnetization curves and to 2.0 K according to in-field DSC measurements, both at magnetic field of 1 T (see the supporting information of reference [11]). This compound is generally regarded as one of the benchmarks for the Fe_2P-type compounds. It can be cycled for 10 thousand times and the sample geometry remains intact. A higher level of B substitution can further decrease ΔT_{hys} but fails to provide a sufficiently large GMCE [17]. It is essential to find a new approach to further decrease ΔT_{hys} and simultaneously provide a sufficiently high GMCE, as characterized by the isothermal magnetic entropy change (ΔS_M) and the adiabatic temperature change (ΔT_{ad}). To evaluate the size of ΔS_M, Gd with a value of ΔS_M is 3 J/kgK under 1 T is generally used as a standard to compare with [18]. Another design criterion is that ΔT_{ad} should be larger than 2.0 K [19], since Engelbrecht and Bahl [20] demonstrated that cooling (and heating) is ineffective when ΔT_{ad} drops below 2.0 K.

On the other hand, the magnetic field currently used in the prototypes of heat pumps are generated by NdFeB permanent magnets, which varies from 0.9 to 1.9 T [21–24]. The overall cost to reach a field of 1.9 T can be 10 times higher than the cost to reach a field of 0.9 T. It is therefore of interest to explore the lower magnetic field potential of the magnetic heat pump system. dT_c/dB is defined as the shift of T_c induced by an applied magnetic field. As the magnitude of dT_c/dB is regarded as the driving force of the magnetoelastic transition [25], if enhanced, the magnetic phase transition can be induced in lower magnetic fields. It is positive for conventional first-order magnetic transition materials, such as $MnFeP_{1-x-y}Si_xB_y$ [11] and La-Fe-Si [26], while it is negative for the inverse first-order magnetic transition materials, for instance the Ni–Mn–X-- Heusler compounds with X = Sn, Sb and In [27] or Fe-Rh [28]. For the conventional first-order magnetic transition materials, this shift is attributed to the magnetic field stabilization of the phase with the higher magnetization, being the low-temperature ferromagnetic phase [13,29]. In an external magnetic field, extra thermal energy is then needed to induce the magnetic phase transition. Thus, T_c shifts to higher temperature. One of our motivations of this work is to increase the driving force (i.e. dT_c/dB) of FOMT and make it feasible to be utilized in devices with low-cost permanent magnets.

In previous reports we have shown an enhanced GMCE in the low magnetic field range by introducing V substitution to Mn-Fe-P-Si compounds [30,31]. From the motivation of minimizing ΔT_{hys} and achieving a large GMCE under a magnetic field of 1.0 T, the combined effect of B and V additions to the Mn-Fe-P-Si compounds is investigated in this study. The effect of V substitution on the thermal hysteresis ΔT_{hys}, the lattice parameters, the magnetic properties and dT_c/dB in polycrystalline Mn-V-Fe-P-Si-B compounds are systematically investigated. Through optimization of the composition and V substitution, an ultra-low ΔT_{hys} of 0.5 K and a large GMCE with $|\Delta S_M|$ = 6.2 J/kgK and ΔT_{ad} = 2.5 K at an internal magnetic field of 1 T is achieved simultaneously.

2. Experimental

Polycrystalline $Mn_{1-x1}V_{x1}Fe_{0.95}P_{0.593}Si_{0.33}B_{0.077}$ (x_1 = 0.00, 0.02, 0.03) compounds were prepared by a powder metallurgy method. The vanadium substitution started from 0.02 since it was reported to be optimal to tune the hysteresis and entropy change in low magnetic fields [30]. The starting materials in the form of Mn, Fe, red P, Si and V powders were mechanically ball milled for 10 h in an Ar atmosphere with a constant rotation speed of 380 rpm, then pressed into small pellets, and finally sealed in quartz ampoules under 200 mbar of Ar before employing the various heat treatment conditions. The pellets were annealed at 1323 K for 2 h to promote crystallization and cooled to room temperature in the furnace. Then they were heated up to the same annealing temperature for 20 h to homogenize the compound and finally quenched in water. This batch samples were labeled as *series A*. In this series, the composition of sample with x_1 = 0.00 is designed to be the same as to the previous benchmark material $MnFe_{0.95}P_{0.595}Si_{0.33}B_{0.075}$ [11]. In order to enhance the $|\Delta S_M|$, an optimal composition series of $Mn_{1-x2}V_{x2}Fe_{0.95}P_{0.563}Si_{0.36}B_{0.077}$ (x_2 = 0.00, 0.02, 0.03) compounds with a higher Si content was prepared with the same procedure as series *A* at a higher annealing temperature of 1373 K. This batch samples are labeled as *series B*.

X-ray diffraction (XRD) patterns were collected on a PANalytical X-pert Pro diffractometer with Cu-K_α radiation (1.54056 Å) at room temperature. The temperature dependence and magnetic field dependence of the magnetization were measured with a commercial superconducting quantum interference device (SQUID) magnetometer (Quantum Design MPMS 5XL) in the reciprocating sample option (RSO) mode. The adiabatic temperature change (ΔT_{ad}) was measured in a Peltier cell based differential scanning calorimeter (DSC) using a Halbach cylinder providing a magnetic field of up to 1.5 T. In this setup, the iso-field calorimetric scans were performed at a rate of 3 K min^{-1}, while the temperature had been corrected for the effect of the thermal resistance of the Peltier cells.

3. Results and discussion

Fig. 1(a) shows the room temperature XRD patterns and the refined results for the $Mn_{1-x2}V_{x2}Fe_{0.95}P_{0.563}Si_{0.36}B_{0.077}$ (x_2 = 0.02) compound. The main phase is identified as the hexagonal Fe_2P-type phase (2:1) with a space group of P-*62 m* and the impurity phase is the cubic $MnFe_2Si$-type phase (3:1) with a space group of F*m3m*, which agrees with the previously reported data [1]. A high weight fraction of 96.3 wt% is obtained for the main phase, suggesting that the annealing condition and composition are suitable to achieve a high purity of Fe_2P-type phase. Based on the refinement results, the weight fraction of the impurity phase is 1.8 ± 0.1, 2.4 ± 0.1 and 2.0 ± 0.1 wt% for x_1 = 0.00, 0.02 and 0.03 and is 4.5 ± 0.1, 3.8 ± 0.1 and 4.3 ± 0.1 wt% for x_2 = 0.00, 0.02 and 0.03, respectively. Thus, the variation in the amount of impurity phase by V substitution is negligible within the same series.

In Fig. 1(b), the results of the Fullprof refinement [32] for the lattice parameters of the *series* A compounds are shown. An increase in V substitution leads to a decrease in *a* axis and an increase in *c* axis. The lattice constant *a* decreases from 6.0459 to 6.0339 Å and *c* increases from 3.3966 to 3.4076 Å when x_1 increases from 0 to 0.03. In Fig. 1(c) and 1(d), the lattice parameters, *c*/*a* ratio and T_C are shown for the *series* B compounds. The lattice constant *a* decreases from 6.0508 to 6.0422 Å and *c* increases from 3.3998 to 3.4063 Å when x_2 is increased from 0 to 0.03, see the Fig. 1(c). The increase in the *c*/*a* ratio leads to a decrease in T_C, as shown in Fig. 1(d). The correlation between the *c*/*a* ratio and T_C originates from the distinct mixed magnetism of the Fe_2P type compounds [33]. The Fe atoms prefer to occupy the plane and Mn atoms prefer to occupy the *3 g* plane with P and Si randomly distributed in the hexagonal lattice. When transforming from the paramagnetic to the ferromagnetic state, the lattice constant *a* increases and causes a stronger localization for the *3d* electrons of Fe (*3f*) instead of chemical bonding with non-metallic P and Si. Jointly with the lattice constant *c*, decreases the interlayer distance between the Mn and Fe atoms and thereby enhances the magnetic exchange interaction between two magnetic atoms [34]. Therefore, adding V to $Mn_{1-x2}V_{x2}Fe_{0.95}P_{0.593}Si_{0.33}B_{0.077}$ compounds will increase the *c*/*a* ratio and leads to a reduction in the magnetic exchange interaction. Similar trend is observed for the $Mn_{1-x1}V_{x1}Fe_{0.95}P_{0.593}Si_{0.33}B_{0.077}$ compounds. As a result, T_C is reduced. These trends are consistent with the previous investigation for the effect of V substitution in the Mn-Fe-P-Si compounds [30].

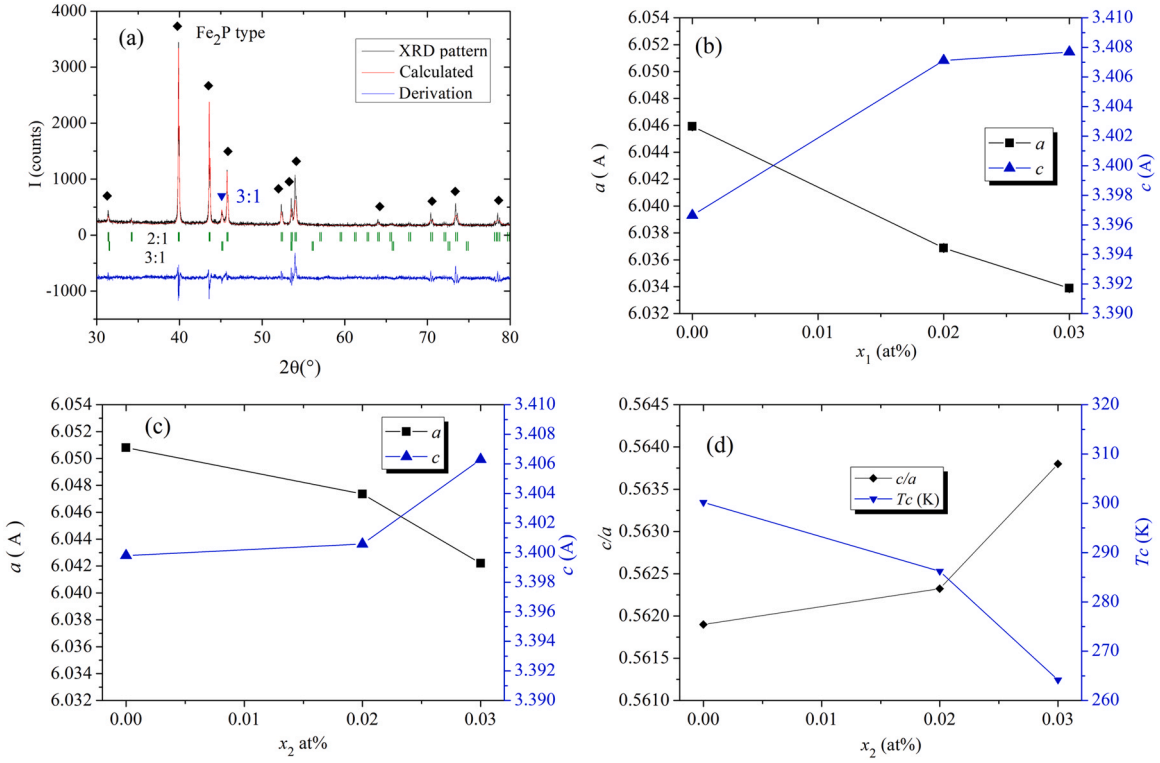

Fig. 1. (a) XRD pattern and the refined results for $Mn_{1-x2}V_{x2}Fe_{0.95}P_{0.563}Si_{0.36}B_{0.077}$ (x_2 = 0.02) compounds; (*b*) Lattice parameters *a* and *c* as function of value of x_1 for $Mn_{1-x1}V_{x1}Fe_{0.95}P_{0.593}Si_{0.33}B_{0.077}$ (*series* A) and (*c*) Lattice parameters *a* and *c* and (*d*) *c*/*a* ratio and T_C as function of value of x_2 for $Mn_{1-x2}V_{x2}Fe_{0.95}P_{0.563}Si_{0.36}B_{0.077}$ (*series* B).

The temperature dependence of the magnetization in the compounds of *series A* and *B* are shown in Fig. 2(a) and 2(b), respectively. For decreasing temperature, they have a temperature-induced magnetic phase transition from paramagnetic to ferromagnetic state. The transition temperature T_C is determined from the maximum value of *-dM/dT* in the *M-T* curve measured during heating at 1 T. For *series A*, T_C tends to decrease with increasing V substitution. When x_1 increases from 0 to 0.02, T_C decreases from 290.0 to 255.2 K. For *series B*, T_C decreases from 300 to 286.2 K when x_2 increases from 0 to 0.02. Thus, T_C in *series B* is tuned to the near room-temperature region, which makes it suitable as a series of working materials for near room temperature applications. The value of *-dM/dT* indicates how strong the FOMT is. The values of *-dM/dT* are 7.6, 5.0 and 3.0 Am^2/kgK for x_1 = 0.00, 0.02 and 0.03 and are 11.1, 5.6 and 5.2 Am^2/kgK for x_2 = 0.00, 0.02 and 0.03, respectively. Thus, *-dM/dT* decreases by increasing V content, i.e. the FOMT is weakened.

The value of ΔT_{hys} is determined by calculating the difference in the maximum value of *-dM/dT* during cooling and heating in an applied magnetic field of $\mu_0 H$ = 1 T at a ramp rate of 2 $Kmin^{-1}$. For *series A*, ΔT_{hys} decreases by 36% from 1.1 to 0.7 K when x_1 increases from 0.00 to 0.03. For *series B*, ΔT_{hys} decreases by 93% from 1.5 to 0.1 K when x_2 increases from 0.00 to 0.03, see Table 1. The *M-H* curves for series *B* are measured under ascending and descending fields around the Curie temperature using a loop process [35]. The magnetic hysteresis is also found to decrease when x_2 increases from 0 to 0.02, as shown in the Fig. S1. Thus, magnetic and thermal hysteresis show the same trend. When a ΔT_{hys} of 0.5 K is achieved, up to 75% of the Carnot efficiency is feasible for the sample with x_2 = 0.02

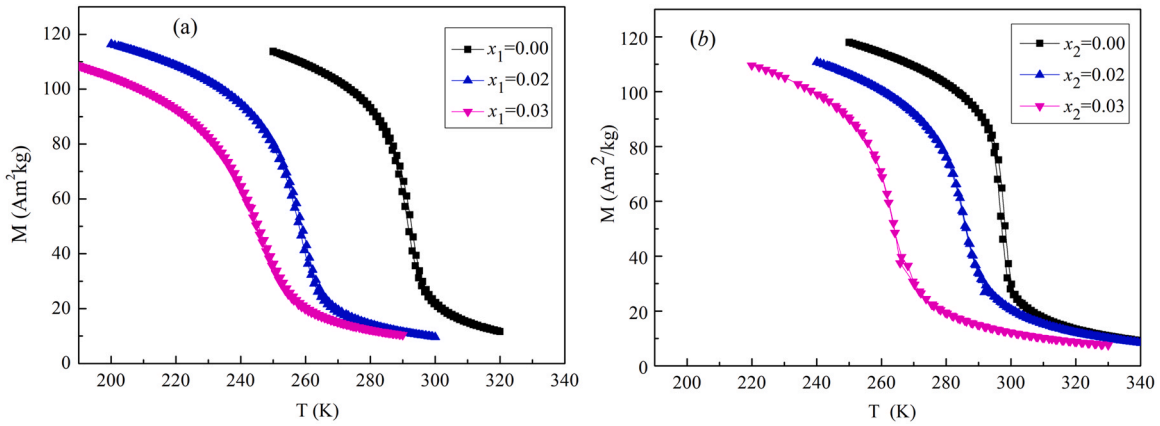

Fig. 2. Temperature dependence of magnetization for (a) $Mn_{1-x1}V_{x1}Fe_{0.95}P_{0.593}Si_{0.33}B_{0.077}$ and (b) $Mn_{1-x2}V_{x2}Fe_{0.95}P_{0.563}Si_{0.36}B_{0.077}$ compounds under an applied magnetic field of 1 T.

Table 1
Curie temperature (T_C), thermal hysteresis (ΔT_{hys}), latent heat (L), magnetic entropy change ($|\Delta S_M|$) and adiabatic temperature change ΔT_{ad} at a field change of 1 T for *series A* and *B*. The value of ΔT_{hys} is determined in an applied magnetic field of $\mu_0 H$ = 1 T at a ramp rate of 2 Kmin^{-1}.

	Annealed T (K)	Sample	T_C (K)	ΔT_{hys} (K)	L (kJ/kg)	$\|\Delta S_M\|$ (J/(kg·K))	ΔT_{ad} (K)
series A	1323	x_1 = 0.00	290.0	1.1	5.2	6.5	2.7
series A	1323	x_1 = 0.02	255.2	0.9	2.4	4.6	1.6
series A	1323	x_1 = 0.03	242.5	0.7	1.7	2.7	/
series B	1373	x_2 = 0.00	300.2	1.5	6.2	11.3	3.5
series B	1373	x_2 = 0.02	286.2	0.5	3.3	5.6	2.3
series B	1373	x_2 = 0.03	264.2	0.1	2.8	4.8	1.6
Ref. [11]	1373	x_1 = 0.00	281	1.6	3.8	9.8	2.5

[14]. The value of ΔT_{hys} is determined by both intrinsic properties, i.e. the strength of the FOMT and extrinsic properties like the fraction of the impurity phase [13]. Here the intrinsic weakening of FOMT is the dominant factor that reduces ΔT_{hys} to an ultra-low value as the compounds have very similar amount of impurity phase within the series.

The latent heat is an important quantity to characterize how strong the FOMT is. The DSC curves for *series A* and *B* are measured under zero field, as shown in the Fig. 3, and the derived latent heat is also listed in Table 1.

In Fig. 3, the DSC curves for *series A* and *B* were measured under zero field. By increasing the V content, the heat capacity is largely decreased, indicating that a strong FOMT is transferred to a weak FOMT. For the sample with x_1 = 0.00 and x_2 = 0.00, sharp heat capacity peaks are shown, indicating a strong FOMT. When increasing V content, the heat capacity is decreased, suggesting the FOMT is weaker. As shown in the Table 1, increasing x_1 from 0.00 to 0.03 results in a strong reduction of the latent heat by 67% from 5.2 to 1.7 J/g for *series A*. Similarly, increasing x_2 from 0.00 to 0.03 results in a strong reduction of the latent heat by 55% from 6.2 to 2.8 J/g (listed in Table 1). The sample with x_2 = 0.02 in series *B* has a slightly lower latent heat of 3.3 J/g than the previous benchmark $MnFe_{0.95}P_{0.595}Si_{0.33}B_{0.077}$ compound of 3.8 J/g [11]. Therefore, the lower latent heat and the high fraction of the Fe_2P-type phase (96.3 wt%) can explain the low value of ΔT_{hys} of 0.5 K found in the sample with x_2 = 0.02.

The iso-thermal entropy change $|\Delta S_M|$ is widely used as a criterion to evaluate the amount of heat transferred in one thermodynamic cycle. The values of $|\Delta S_M|$ are derived from iso-field magnetization curves using the Maxwell relation [36,37]. The iso-field magnetization curves of *series A* and *B* for a magnetic field change are measured in the vicinity of T_C with a temperature interval of 1 K. In order to minimize the effect of demagnetization factor, the applied magnetic field starts from 0.6 T and increases to 2 T in a step of 0.1 T. The calculated temperature dependence of $|\Delta S_M|$ for *series A* and *B* are shown in Fig. 4(*a*) and 4(*c*), respectively. The values of $|\Delta S_M|$ are 5.9, 4.5, 2.7 J/(kgK) at 1 T and 10.5, 8.0, 5.5 J/(kgK) at 2.0 T for samples with x_1 = 0, 0.02, and 0.03, respectively. Note that the GMCE of the compound with x_1 = 0.00 is lower than the previous benchmark compound for Mn-Fe-P-Si-B [11] ($|\Delta S_M|$ = 9.2 J/(kgK) at 1 T), which is due to the decrease of annealing temperature from 1373 to 1323 K.In *series B*, values of $|\Delta S_M|$ are 11.3, 5.6, 4.8 J/(kgK) at 1 T and 14.9, 8.4, 8.0 J/(kgK) at 2.0 T for samples with x_2 = 0, 0.02, and 0.03, respectively. After increasing the Si content from 0.33 to 0.36, $|\Delta S_M|$ of the sample with x_2 = 0.00 in *series B* outperforms the previously benchmark compound for Mn-Fe-P-Si-B [11]. This provides some room for V substitution to decrease ΔT_{hys}, while retaining a large $|\Delta S_M|$. When x_2 increases to 0.02, $|\Delta S_M|$ is reduced to 5.6 J/(kgK) at 0–1 T, which is still about two times larger than that of polycrystalline Gd ($|\Delta S_M|$ = 3.0 J/(kgK) [18].

In the magnetocaloric properties, ΔT_{ad} illustrates the direct temperature span that can be achieved in the magnetic heat pump. In-field DSC measurements were conducted at a rate of 3 Kmin^{-1} in the temperature range of 240–340 K. From these measurements, $|\Delta S_M|$ and C_P were collected under a constant magnetic field ($\mu_0 H$ = 0, 0.5, 1.0 and 1.5 T). The values of ΔT_{ad} were calculated by the following equation: [38].

$$\Delta T_{ad} = -\left[\frac{T}{C(T)_{H_F}} S_M(T)_{H_F} - \frac{T}{C(T)_{H_I}} S_M(T)_{H_I}\right] \quad (1)$$

Fig. 4(*b*) illustrates the temperature dependence of the in-field DSC values of ΔT_{ad} for *series A* (x_1 = 0.00 and 0.02) while Fig. 4(*d*) illustrates the temperature dependence of ΔT_{ad} for *series B* (x_2 = 0.00, 0.02 and 0.03). In the *series A*, when x_1 increases from 0.00 to 0.02 at %, the value of ΔT_{ad} decreases from 2.7 to 1.6 K under an applied magnetic field of 1 T. This value of ΔT_{ad} for the benchmark Mn-Fe-P-Si-B [11] was 2.5 K. In the *series B*, when x_2 increases from 0.00 to 0.02, its value of ΔT_{ad} is decreased from 3.5 to 2.3 K at 1 T. At 1.5 T, the value of ΔT_{ad} for the sample with x_2 = 0.02 is 3.2 K. Thus, ΔT_{ad} for the sample of x_2 = 0.02 is sufficiently high to be utilized in a device, since cooling (and heating) may be effective when one achieves ΔT_{ad} above 2.0 K [19].

The question is why the low hysteresis and high entropy change occurs in the sample with x_2 = 0.02. A quantitative criterion to determine the order of magnetic phase transitions through magnetocaloric curves has been proposed recently, i.e. the field exponent $n = d\ln(|\Delta S_M|)/d\ln(H)$ for the relative field dependence of magnetic entropy change shows a maximum of $n > 2$ near the transition

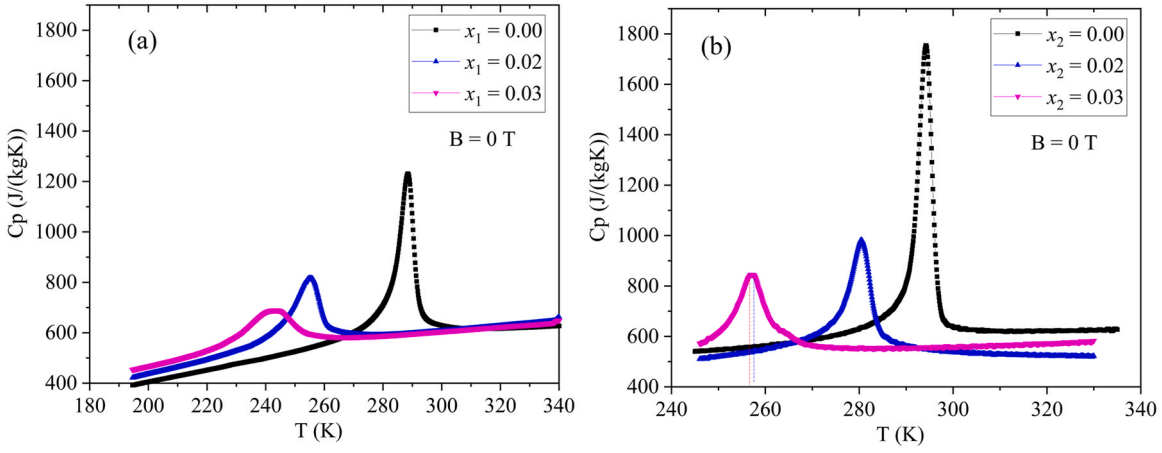

Fig. 3. Heating DSC curves of *series A* and *B* are measured under zero field.

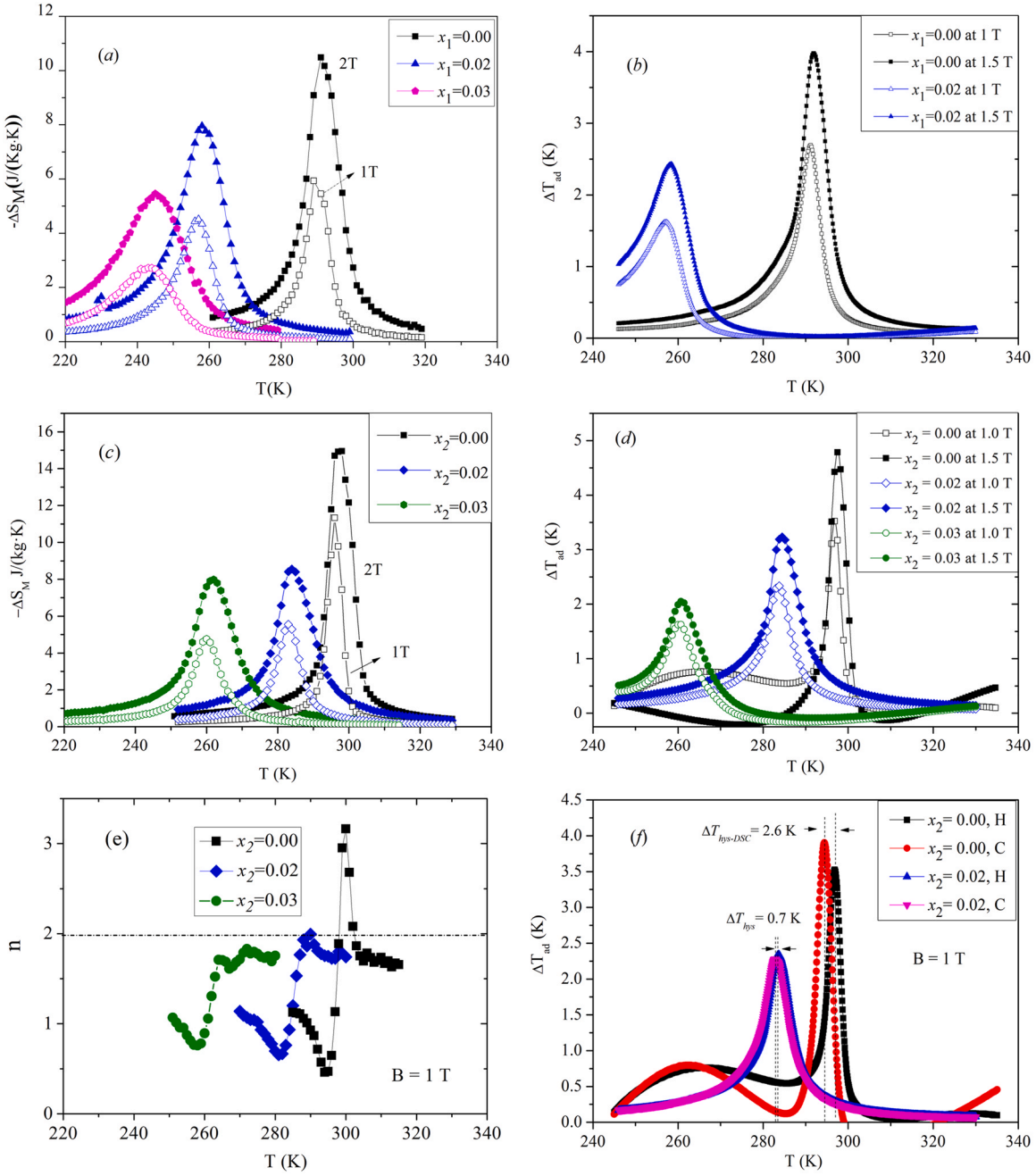

Fig. 4. (*a*) and (*c*) Temperature dependence of $|\Delta S_M|$ under a field change of 0–1.0 T (open symbols) and 0–2.0 T (filled symbols) for *series A* and *B*, respectively; (*b*) and (*d*) Temperature dependence of ΔT_{ad} under a field change of 0–1.0 T (open symbols) and 0–1.5 T (filled symbols) during heating for *series A* and *B*, respectively; (*e*) Temperature dependence of the field exponent $n = d\ln(|\Delta S_M|)/d\ln(H)$ under a field change of 1.0 T for x_2 = 0 and 0.02; (*f*) Temperature dependence of ΔT_{ad} under a field change of 0–1.0 T during heating and cooling for *series B*.

temperatures for a FOMT, while the absence of such overshoot indicates a SOMT [39,40]. For the critical composition, the minimum value of n corresponds to 0.4 [40–42]. The temperature dependence of the field exponent n under a field change of 1.0 T for x_2 = 0 and 0.02 is shown in Fig. 4(e). For x_2 = 0 sample, a clear distinct overshoot of $n > 2$ is observed near its transition temperature, which indicates it is a FOMT. Due to the presence of impurity (3:1) phase (observed from XRD results) in the samples, which itself exhibits a T_C= 575 ºC, [43] n decreases to values below 2 after the overshoot (the typical n value for paramagnetic state is 2) due to the ferromagnetic state of the existing (3:1) phase. It corresponds to the composition nearest to critical point of the FOMT and SOMT for x_2 = 0.02, since it is in good agreement with the shape of n for critical point proposed in reference [39]. However, the presence of impurities can affect the absolute value of n, decreasing below the expected value of 2 for impurity phases with larger Curie temperatures. The observed slight increase of n to values close to 2 followed by a decrease might be an indication of a combined effect of a weakly first order phase transition and the presence of such impurities, which agrees with microstructural observations and the presence of a small thermal hysteresis. Accordingly, a good combination of low hysteresis and high entropy change can be obtained in this compound. For x_2 = 0.03, the minimum of n near the transition is rather shallow and two peaks are shown when passing the transition temperature. This type of shape for the field exponent n indicates that it has phase separation of Fe_2P-type structure, which agrees with the two peaks of

zero-field DSC in the Fig. 3. As shown in the Fig. S2, the phase separation of the Fe_2P-type phase is observed for x_2 = 0.03. There are two peaks in the DSC curves, which show an interval of transition temperature about 1 K. The zero-hysteresis is shown in the M-T curve of x_2 = 0.03 but is not shown for its in-field DSC data. The reason for the different value of hysteresis for M-T and DSC measurement is not clear yet. Recently, the origins for zero-hysteresis in the materials with IEM are investigated from the aspect of nanoscale phase separation [6,44,45] and the secondary phases [46]. Thus, we propose an explanation based on the in-field DSC data. Note that the T_{peak} of heating DSC curve for phase 1 and cooling DSC curve for phase 2 are overlapped. When the paramagnetic phase is transferred to ferromagnetic phase, the phase 1 with higher T_c will become ferromagnetic first and then the stray field [46] from this ferromagnetic phase can assist the phase transition of paramagnetic phase 2. As a result, the phase separation helps to achieve zero-hysteresis in M-T curves. Nevertheless, the phase separation may not be a good strategy for get a GMCE since it will also scarify the $|\Delta S_M|$ and ΔT_{ad}, see Fig. 4 (*c*) and (*d*) and shows hysteresis in the DSC measurement.

In addition, $\Delta T_{hys\text{-}DSC}$ is determined by the difference of the heating and cooling process for the in-field DSC under a field change of 1 T measured at a rate of 3 $Kmin^{-1}$, as shown in Fig. 4(*f*). It differs from the ΔT_{hys} calculated by the *M-T* curves at a rate of 2 $Kmin^{-1}$. Due to the thermal-lag effect, a higher measuring rate leads to a higher ΔT_{hys}, as demonstrated for the Eu_2In compound [47]. In *series B*, $\Delta T_{hys\text{-}DSC}$ decreases from 2.4 to 0.7 K when x_2 increases from 0.00 to 0.02, see Fig. 4(*f*). The value of ΔT_{ad} for $Mn_{0.98}V_{0.02}Fe_{0.95}P_{0.563}Si_{0.36}B_{0.077}$ (ΔT_{ad} = 2.3 K) in *series B* is competitive to that of $MnFe_{0.95}P_{0.563}Si_{0.36}B_{0.077}$ compound (ΔT_{ad} = 2.5 K) [11], but its value for $\Delta T_{hys\text{-}DSC}$ is reduced by 85%. Thus, it is promising to achieve a large value of ΔT_{ad} and an ultra-low $\Delta T_{hys\text{-}DSC}$, which can significantly improve the heat exchange efficiency of the magnetic cooling (and heating) system.

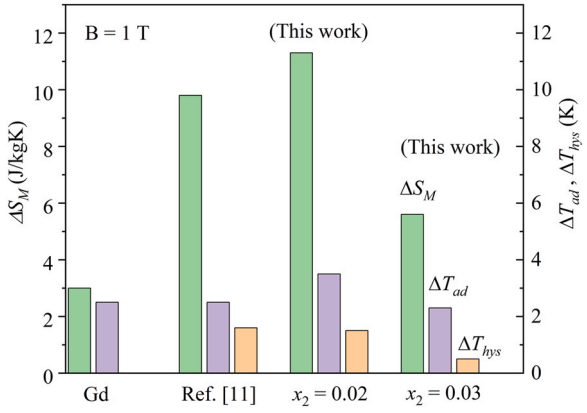

Fig. 5. Figure of merit of $|\Delta S_M|$, ΔT_{ad} and ΔT_{hys} for Gd [18], $MnFe_{0.95}P_{0.563}Si_{0.36}B_{0.077}$ [11], $MnFe_{0.95}P_{0.563}Si_{0.36}B_{0.077}$ and $Mn_{0.98}V_{0.02}Fe_{0.95}P_{0.563}Si_{0.36}B_{0.077}$ *in series B*.

The summary of maximum values for $|\Delta S_M|$, ΔT_{ad} and ΔT_{hys} at a magnetic field of 1.0 T for Gd, $MnFe_{0.95}P_{0.563}Si_{0.36}B_{0.077}$, $MnFe_{0.95}P_{0.563}Si_{0.36}B_{0.077}$ (this work) and $Mn_{0.98}V_{0.02}Fe_{0.95}P_{0.563}Si_{0.36}B_{0.077}$ (this work) is shown in Fig. 5, demonstrating the merit of the compounds in this work. The value of ΔT_{ad} for x_2 = 0.02 is 2.3 K, comparable to 2.8 K of polycrystalline Gd, but its $|\Delta S_M|$ is almost twice larger than Gd [18]. Accordingly, the coefficient of refrigerant performance (*RCP*) = $\frac{\Delta S^* \Delta T_{ad}}{\int_0^B M(Tc,B)dB}$ of the sample with x_2 = 0.02 is calculated to be 0.47, larger than Gd (*RCP* = 0.17) and $Fe_{0.49}Rh_{0.51}$ (*RCP* = 0.22) [48]. Thus, the $MnFe_{0.95}P_{0.563}Si_{0.36}B_{0.077}$ (x_2 = 0.00) and $Mn_{0.98}V_{0.02}Fe_{0.95}P_{0.563}Si_{0.36}B_{0.077}$ (x_2 = 0.02) are clearly good candidates for magnetic heat pumps operating near room temperature.

To investigate the reason why V deceases the hysteresis without losing the GMCE, the effect of V on dT_C/dB is investigated. The magnetic field dependence of T_C and dT_C/dB for *series B* are shown in Fig. 6(a). The value of dT_C/dB increases from 4.0 to 4.8 K/T when the V content is changed from x_2 = 0.00 to x_2 = 0.02. This is comparable to the dT_C/dB value for $(Mn,Fe)_2(P,As)$ compounds, where dT_C/dB was found to be 5.2 K/T [49]. The Clausius–Clapeyron relation for a FOMT corresponds to $dT_C/dB = -T_C\Delta M/L$, where B is the applied magnetic field and ΔM is the jump in magnetization. Thus, the increase in dT_C/dB is mainly caused by the decrease in latent heat (see Table 1), since the values of T_C and ΔM are reduced (see Fig. 2). The increase in dT_C/dB suggests that the driving force for the FOMT is enhanced. As a result, a strong field response is found for low fields, as shown in the magnetization curve of x_2 = 0.02 in the Fig. 6(b).

From the saturation magnetization displayed in Fig. 6(b), the value of the magnetic moment per formula unit ($\mu_{f.u.}$) for *series B* was calculated, as mentioned in reference [50]. For *series B*, the value of $\mu_{f.u.}$ increases from 3.75 to 3.96 $\mu_B/_{f.u.}$ when x_2 increases from 0.00 to 0.02. A larger value of $\mu_{f.u.}$ suggests a larger contribution to $|\Delta S_M|$. This agrees with the strengthening effect of V substitution on the magnetic moment formation in the Mn-Fe-P-Si-V compounds [31]. The higher values for dT_C/dB and $\mu_{f.u.}$ illustrate why an ultra-low thermal hysteresis and a GMCE can be achieved simultaneously in the compounds with 0.02 at% V substitution for Mn in *series B*. Thus, introducing V as a new substitutional element is found to be capable of increasing both dT_C/dB and $\mu_{f.u.}$. and thereby decreasing the hysteresis without losing the GMCE.

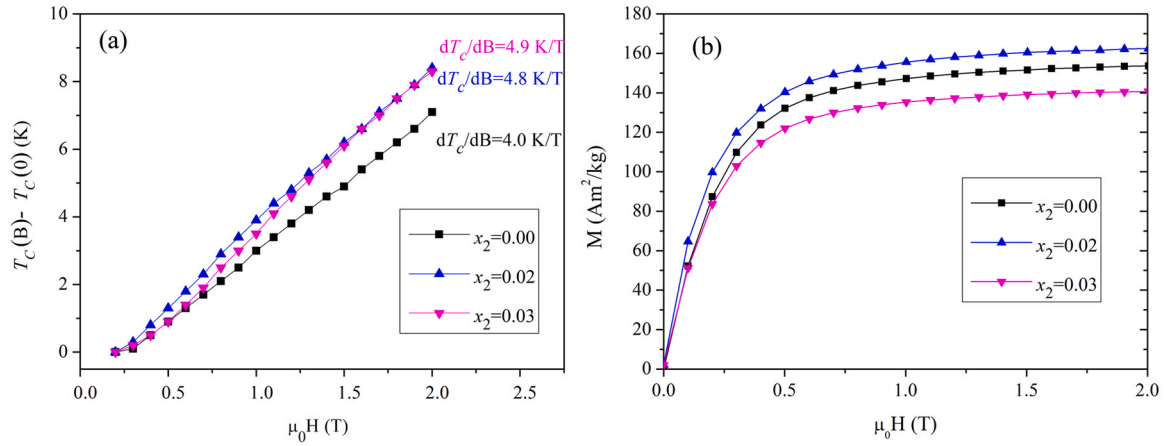

Fig. 6. Field dependence of T_C and dT_C/dB (insets); (b) The magnetization as a function of the V content for *series B* measured at a temperature of 5 K.

4. Conclusions

The ultra-low hysteresis and GMCE of optimal $Mn_{1-x2}V_{x2}Fe_{0.95}P_{0.563}Si_{0.36}B_{0.077}$ compounds pave a pathway to highly efficient magnetic heat pump applications. When x_2 increases from 0.00 to 0.02, the latent heat can be reduced by 55% from 6.2 to 3.3 J/g and thus ΔT_{hys} decreases by 67% from 1.5 to 0.5 K, the $|\Delta S_M|$ is decreased from 11.3 to 5.6 J/kgK and the ΔT_{ad} is decreased from 3.5 to 2.3 K at 1 T. The optimal composition of x_2 = 0.02 is proven to be close to the critical point between the FOMT and the SOMT. The combination of increase in dT_C/dB and increase in magnetic moment $\mu_{f.u.}$ of $Mn_{0.98}V_{0.02}Fe_{0.95}P_{0.563}Si_{0.36}B_{0.077}$ compound can provide a sufficiently large GMCE and an ultra-low value (0.5 K) of ΔT_{hys}. Thus, the coefficient of refrigerant performance (CRP) of this compound is two times larger than Gd. The current $Mn_{1-x}V_xFe(P,Si,B)$ compounds provide an excellent candidate for designing materials towards magnetic heat pump applications using low-cost permanent magnets near-room temperature. The mechanical properties and thermal conductivity of the $Mn_{1-x2}V_{x2}Fe_{0.95}P_{0.563}Si_{0.36}B_{0.077}$ compounds will need to be investigated further to demonstrate the full potential for future utilization in practical devices.

CRediT authorship contribution statement

Ekkes Brück: Conceptualization, Methodology, Reviewing. **Jiawei Lei**: Data curation, Writing – original draft. **Xinmin You**: Data curation, Writing. **Jiayan Law**: Data curation, Writing. **Victorino Franco**: Data curation, Writing. **Bowei Huang**: Data curation, Writing. **Dimitrios Bessas**: Data curation, Writing. **Michael Maschek**: Data curation, Writing. **Dechang Zeng**: Supervision, Methodology, Reviewing. **Niels van Dijk**: Visualization, Investigation, Writing – review & editing.

Data availability

Data will be made available on request.

Declaration of Competing Interest

The authors declare the following financial interests/personal relationships which may be considered as potential competing interests: Jiawei Lai, Victorino Franco reports financial support was provided by Guangzhou ethics project. Michael Maschek reports financial support was provided by EIT Climate KIC. Ekkes Bruck has patent #P1600096NL00 pending to Technische Universiteit Delft. Jiawei Lai has patent #P1600096NL00 pending to Technische Universiteit Delft.

Acknowledgements

The authors acknowledge Anton Lefering, Kees Goubitz, L. Zhang, and Bert Zwart for their technical assistance. The authors also thank Yibole for fruitful discussions. This work is financially supported by the Dutch Science Foundation NWO under applied sciences project 14013. This work is also supported by Guangdong Provincial Science and Technology Program (Grant No. 2015A050502015), the Guangzhou Municipal Science and Technology Program (No. 201505041702137), Natural Science Foundation of the Guangdong Province (2016A030313494), and Zhongshan Municipal Science and Technology Program (Platform construction and innovation team). The author thanks for the financial support of the Guangzhou Ethics Project. V.F. and J.Y.L. acknowledge the financial support of AEI/FEDER-UE (grant PID2019-105720RB-I00). M.M. acknowledges financial support from EIT Climate KIC project “Local, magnetocaloric power conversion opportunities for Cities” (ID 210045).

Appendix A. Supporting information

Supplementary data associated with this article can be found in the online version at doi:10.1016/j.jallcom.2022.167336.

References

[1] E. Brück, O. Tegus, D.T.C. Thanh, K.H.J. Buschow, Magnetocaloric refrigeration near room temperature (invited), J. Magn. Magn. Mater. 310 (2007) 2793–2799.
[2] V. Franco, J.S. Blázquez, J.J. Ipus, J.Y. Law, L.M. Moreno-Ramírez, A. Conde, Magnetocaloric effect: from materials research to refrigeration devices, Prog. Mater. Sci. 93 (2018) 112–232.
[3] V.K. Pecharsky, K.A. Gschneidner, Giant magnetocaloric effect in $Gd_5(Si_2Ge_2)$, Phys. Rev. Lett. 23 (1997) 4494–4497.
[4] F.X. Hu, B.G. Shen, J.R. Sun, Z.H. Cheng, Influence of negative lattice expansion and metamagnetic transition on magnetic entropy change in the compound $LaFe_{11.4}Si_{1.6}$, Appl. Phys. Lett. 23 (2001) 3675–3677.
[5] S. Fujieda, A. Fujita, K. Fukamichi, Large magnetocaloric effect in $La(Fe_xSi_{1-x})_{13}$ itinerant-electron metamagnetic compounds, Appl. Phys. Lett. 81 (2002) 1276–1278.
[6] Y. Liu, X. Fu, Q. Yu, M. Zhang, J. Liu, Significant reduction of phase-transition hysteresis for magnetocaloric $(La_{1-x}Ce_x)_2Fe_{11}Si_2H_y$ alloys by microstructural manipulation, Acta Mater. 207 (2021) 116687.
[7] J. Liu, M. Krautz, K. Skokov, T.G. Woodcock, O. Gutfleisch, Systematic study of the microstructure, entropy change and adiabatic temperature change in optimized La–Fe–Si alloys, Acta Mater. 9 (2011) 3602–3611.
[8] O. Tegus, E. Brück, K.H.J. Buschow, F.R. de Boer, Transition-metal-based magnetic refrigerants for room-temperature applications, Nature 415 (2002) 150–152.
[9] N.H. Dung, Z.Q. Ou, L. Caron, L. Zhang, D.T. Cam Thanh, K.H.J. Buschow, E. Brück, Mixed magnetism for refrigeration and energy conversion, Adv. Energy Mater. 6 (2011) 1215–1219.
[10] N.H. Dung, L. Zhang, Z.Q. Ou, K.H.J. Buschow, Magnetoelastic coupling and magnetocaloric effect in hexagonal Mn–Fe–P–Si compounds, Scr. Mater. 12 (2012) 975–978.
[11] F. Guillou, G. Porcari, H. Yibole, N.H. van Dijk, E. Brück, Taming the first-order transition in giant magnetocaloric materials, Adv. Mater. 17 (2014) 2671–2675.
[12] S.K. Pal, C. Frommen, S. Kumar, B.C. Hauback, H. Fjellvåg, G. Helgesen, Enhancing giant magnetocaloric effect near room temperature by inducing magnetostructural coupling in Cu-doped MnCoGe, Mater. Des. 195 (2020) 109036.
[13] N. Trung, L. Zhang, L. Caron, K. Buschow, E. Brück, Giant magnetocaloric effects by tailoring the phase transitions, Appl. Phys. Lett. 96 (2010) 172504.
[14] J. Liu, T. Gottschall, K.P. Skokov, J.D. Moore, O. Gutfleisch, Giant magnetocaloric effect driven by structural transitions, Nat. Mater. 11 (2012) 620.
[15] N.H. Dung, Z.Q. Ou, L. Caron, L. Zhang, D.T.C. Thanh, G.A. de Wijs, R.A. de Groot, K.H.J. Buschow, E. Brück, Mixed magnetism for refrigeration and energy conversion, Adv. Energy Mater. 1 (2011) 1215–1219.
[16] T.D. Brown, T. Buffington, P.J. Shamberger, Effects of hysteresis and Brayton cycle constraints on magnetocaloric refrigerant performance, J. Appl. Phys. 123 (2018) 185101.
[17] F. Guillou, H. Yibole, G. Porcari, L. Zhang, N.H. van Dijk, E. Brück, Magnetocaloric effect, cyclability and coefficient of refrigerant performance in the MnFe(P,Si,B) system, J. Appl. Phys. 116 (2014) 063903.
[18] S.V. Taskaev, M.D. Kuz'min, K.P. Skokov, D.Y. Karpenkov, A.P. Pellenen, V.D. Buchelnikov, O. Gutfleisch, Giant induced anisotropy ruins the magnetocaloric effect in gadolinium, J. Magn. Magn. Mater. 331 (2013) 33–36.
[19] J. Lyubina, Magnetocaloric materials for energy efficient cooling, J. Phys. D Appl. Phys. 50 (2017) 053002.
[20] K. Engelbrecht, C.R.H. Bahl, Evaluating the effect of magnetocaloric properties on magnetic refrigeration performance, J. Appl. Phys. 108 (2010) 123918.
[21] R. Bjørk, C.R.H. Bahl, A. Smith, N. Pryds, Review and comparison of magnet designs for magnetic refrigeration, Int. J. Refrig. 33 (2010) 437–448.
[22] B.F. Yu, Q. Gao, B. Zhang, X.Z. Meng, Z. Chen, Review on research of room temperature magnetic refrigeration, Int. J. Refrig. 26 (2003) 622–636.
[23] Z.G. Zheng, H.Y. Yu, X.C. Zhong, D.C. Zeng, Z.W. Liu, Design and performance study of the active magnetic refrigerator for room-temperature application, Int. J. Refrig. 32 (2009) 78–86.
[24] M. Krautz, L. Beyer, A. Funk, A. Waske, B. Weise, J. Freudenberger, T. Gottschall, Predicting the dominating factors during heat transfer in magnetocaloric composite wires, Mater. Des. 193 (2020) 108832.
[25] T. Faske, I.A. Radulov, M. Hölzel, O. Gutfleisch, W. Donner, Direct observation of paramagnetic spin fluctuations in $LaFe_{13-x}Si_x$, J. Phys. Condens. Matter 32 (2019) 115802.
[26] A. Fujita, S. Fujieda, Y. Hasegawa, K. Fukamichi, Itinerant-electron metamagnetic transition and large magnetocaloric effects in compounds and their hydrides, Phys. Rev. B 67 (2003) 104416.
[27] Y. Sutou, Y. Imano, N. Koeda, T. Omori, R. Kainuma, K. Ishida, K. Oikawa, Magnetic and martensitic transformations of ferromagnetic shape memory alloys, Appl. Phys. Lett. 85 (2004) 4358–4360.
[28] S.A. Nikitin, G. Myalikgulyev, A.M. Tishin, M.P. Annaorazov, K.A.A.L. Asatryan, Tyurin. The magnetocaloric effect in $Fe_{49}Rh_{51}$ compound, Phys. Lett. A 148 (1990) 363–366.
[29] H.E. Karaca, I. Karaman, B. Basaran, Y. Ren, Y.I. Chumlyakov, H.J. Maier, Magnetic field-induced phase transformation in NiMnCoIn magnetic shape-memory

alloys-a new actuation mechanism with large work output, Adv. Funct. Mater. 19 (2009) 983–998.
[30] J. Lai, B. Huang, X. Miao, N. Van Thang, X. You, M. Maschek, L. van Eijck, D. Zeng, N. van Dijk, E. Brück, Combined effect of annealing temperature and vanadium substitution for mangetocaloric $Mn_{1.2-x}V_xFe_{0.75}P_{0.5}Si_{0.5}$ alloys, J. Compd. Compd. 803 (2019) 671–677.
[31] J. Lai, X. You, I. Dugulan, B. Huang, J. Liu, M. Maschek, L. van Eijck, N. van Dijk, E. Brück, Tuning the magneto-elastic transition of $(Mn,Fe,V)_2(P, Si)$ alloys to low magnetic field applications, J. Compd. Compd. 821 (2020) 153451.
[32] H. Rietveld, A profile refinement method for nuclear and magnetic structures, J. Appl. Crystallogr. 2 (1969) 65–71.
[33] N.H. Dung, L. Zhang, Z.Q. Ou, L. Zhao, L. van Eijck, A.M. Mulders, M. Avdeev, E. Suard, N.H. van Dijk, E. Brück, High/low-moment phase transition in hexagonal Mn-Fe-P-Si compounds, Phys. Rev. B 86 (2012) 045134.
[34] X.F. Miao, S.-Y. Hu, F. Xu, E. Brück, Overview of magnetoelastic coupling in (Mn, Fe) 2 (P, Si)-type magnetocaloric materials, Rare Met. 37 (2018) 723–733.
[35] L. Caron, Z.Q. Ou, T.T. Nguyen, D.T. Cam Thanh, O. Tegus, E. Brück, On the determination of the magnetic entropy change in materials with first-order transitions, J. Magn. Magn. Mater. 321 (2009) 3559–3566.
[36] K.A. Gschneidner Jr., V.K. Pecharsky, A.O. Tsokol, Recent developments in magnetocaloric materials, Rep. Prog. Phys. 68 (2005) 1479.
[37] J.S. Blázquez, V. Franco, A. Conde, T. Gottschall, K.P. Skokov, O. Gutfleisch, A unified approach to describe the thermal and magnetic hysteresis in Heusler alloys, Appl. Phys. Lett. 109 (2016) 122410.
[38] K. Ahn, V.K. Pecharsky, K.A. Gschneidner, The magnetothermal behavior of mixed-valence Eu_3O_4, J. Appl. Phys. 106 (2009) 043918.
[39] J.Y. Law, V. Franco, L.M. Moreno-Ramírez, A. Conde, D.Y. Karpenkov, I. Radulov, K.P. Skokov, O. Gutfleisch, A quantitative criterion for determining the order of magnetic phase transitions using the magnetocaloric effect, Nat. Commun. 9 (2018) 2680.
[40] N.H. van Dijk, Landau model evaluation of the magnetic entropy change in magnetocaloric materials, J. Magn. Magn. Mater. 529 (2021) 167871.
[41] C. Romero-Muñiz, V. Franco, A. Conde, Two different critical regimes enclosed in the Bean–Rodbell model and their implications for the field dependence and universal scaling of the magnetocaloric effect, Phys. Chem. Chem. Phys. 19 (2017) 3582–3595.
[42] V. Franco, J.Y. Law, A. Conde, V. Brabander, D.Y. Karpenkov, I. Radulov, K. Skokov, O. Gutfleisch, Predicting the tricritical point composition of a series of LaFeSi magnetocaloric alloys via universal scaling, J. Phys. D Appl. Phys. 50 (2017) 414004.
[43] T. Shinjo, Y. Nakamura, N. Shikazono, Magnetic study of Fe_3Si and Fe_5Si_3 by Mössbauer effect, J. Phys. Soc. Jpn. 18 (1963) 797–801.
[44] A. Fujita, Influence of electronic and metallographic structures on hydrogen redistribution in La(Fe,Si)13-based magnetocaloric compounds, Acta Mater. 169 (2019) 162–171.
[45] D. Huang, T. Ma, D.E. Brown, S.H. Lapidus, Y. Ren, J. Gao, Nanoscale phase separation and large refrigerant capacity in magnetocaloric material $LaFe_{11.5}Si_{1.5}$, Chem. Mater. 33 (2021) 2837–2846.
[46] J. Lai, H. Sepehri-Amin, X. Tang, J. Li, Y. Matsushita, T. Ohkubo, A.T. Saito, K. Hono, Reduction of hysteresis in $(La_{1-x}Ce_x)_y(Mn_zFe_{11.4-z})Si_{1.6}$ magnetocaloric compounds for cryogenic magnetic refrigeration, Acta Mater. 220 (2021) 117286.
[47] F. Guillou, A.K. Pathak, D. Paudyal, Y. Mudryk, F. Wilhelm, A. Rogalev, V.K. Pecharsky, Non-hysteretic first-order phase transition with large latent heat and giant low-field magnetocaloric effect, Nat. Commun. 9 (2018) 2925.
[48] E. Brück, H. Yibole, L. Zhang, A universal metric for ferroic energy materials, Philos. Trans. Ser. A Math. Phys. Eng. Sci. 374 (2016) 2074.
[49] H. Yibole, F. Guillou, L. Zhang, N.H. van Dijk, E. Brück, Direct measurement of the magnetocaloric effect in MnFe (P, X)(X= As, Ge, Si) materials, J. Phys. D Appl. Phys. 47 (2014) 075002.
[50] J.W. Lai, Z.G. Zheng, R. Montemayor, X.C. Zhong, Z.W. Liu, D.C. Zeng, Magnetic phase transitions and magnetocaloric effect of $MnCoGe_{1-x}Si_x$, J. Magn. Magn. Mater. 372 (2014) 86.